

Received 22 July 2022, accepted 18 August 2022, date of publication 25 August 2022, date of current version 2 September 2022.

Digital Object Identifier 10.1109/ACCESS.2022.3201644

RESEARCH ARTICLE

Low-Profile Interdigitated UHF RFID Tag Antenna for Metallic Objects

FUAD ERMAN¹, DALIA MANSOUR², MOHAMMAD KOUALI², ARAFAT SHABANEH³, LEIFUR LEIFSSON⁴, SLAWOMIR KOZIEL^{1,5}, (Fellow, IEEE), ENG-HOCK LIM⁶, (Senior Member, IEEE), AND EFFARIZA HANAFI⁷, (Member, IEEE)

¹Engineering Optimization & Modeling Center, Reykjavik University, 101 Reykjavik, Iceland

²Electronics and Communication Engineering Department, Al-Quds University, Jerusalem 51000, Palestine

³Department of Communication Engineering Technology, Faculty of Engineering and Technology, Palestine Technical University-Kadoorie (PTUK), Tulkarm P304, Palestine

⁴School of Aeronautics and Astronautics, Purdue University, West Lafayette, IN 47907, USA

⁵Faculty of Electronics, Telecommunications and Informatics, Gdansk University of Technology, 80-233 Gdansk, Poland

⁶Electrical and Electronic Engineering Department, Universiti Tunku Abdul Rahman, Bandar Sungai Long, Kajang 43000, Malaysia

⁷Department of Electrical Engineering, Universiti Malaya, Kuala Lumpur 50603, Malaysia

Corresponding author: Fuad Erman (fuadnae@gmail.com)

This work was supported in part by the Icelandic Centre for Research [Rannsóknamiðstöð Íslands (RANNIS)] under Grant 174573, in part by the National Science Centre of Poland under Grant 2018/31/B/ST7/02369, and in part by the Palestine Technical University-Kadoorie (PTUK).

ABSTRACT This paper presents a novel miniature interdigitated ultra-high frequency (UHF) radio frequency identification (RFID) tag antenna that can be placed on metallic objects. The tag structure comprises two horizontal strip lines, each loaded with seven identical open stubs, and an integrated circuit (IC) chip connected directly to the feed lines in the middle of the structure. The perfect match to the IC chip's impedance is realized by adjusting the length of the loaded open stubs and the spaces between the stubs. Molding the antenna's geometry can be applied to realize conjugated impedance with any sort of IC chip due to the flexibility of the tag structure. It is fabricated on a single Polytetrafluoroethylene (PTFE) substrate. Moreover, the proposed structure does not involve any metallic vias or shorting walls, which makes its construction simple and suitable for mass production. The tag of the size of $55.2\text{mm} \times 44.2\text{mm} \times 1.5\text{mm}$ yields a total realized gain of -4.11 dB at the North American band ($902 - 928\text{ MHz}$) while being placed on a $20\text{cm} \times 20\text{cm}$ metallic plate. The measured detection distance is 8.14 m on metallic objects and 5 m in the free space. A good match between the measured and simulated results is observed.

INDEX TERMS Impedance matching, interdigitated structure, metal mountable tag antenna, miniature UHF tag antenna.

I. INTRODUCTION

Nowadays, ultra-high frequency (UHF) radio frequency identification (RFID) technology is widely implemented due to its diverse advantages. Exemplary applications include retail, inventory management, and patient monitoring. From the practical perspective it is preferable to realize tags that can be mounted onto different materials while ensuring appropriate functionality. However, the nature of the tagged surface affects the performance of the tag. This effect is pronounced in the case of tagging metallic surface, where

The associate editor coordinating the review of this manuscript and approving it for publication was Yang Yang¹.

the desired surface current of tag deteriorates and affects the gain, input impedance, antenna efficiency, etc. [1], [3]. Hence, designing a small low-profile tag that can be applied to metallic objects while maintaining its performance, is still a challenge.

In the literature, different approaches have been investigated to overcome the presence of metallic structure. The artificial magnetic conductor (AMC) substrate with an offset of metallic vias is utilized to improve the tag's performance (gain/read range) [4], [7]. The slab of AMC possesses a high dielectric constant and an air gap or foam separated between the meandered dipole antenna and AMC substrate. In addition, the employment of electromagnetic bandgap

(EBG) could prevent the impedance mismatch and the tag's gain G_a is also improved [8]. The EBG structure has been employed as three-layer mushroom-like EBG material [9], EBG cells surrounding the antenna with metallic vias [10], or by etching a lattice of circular slots in the EBG ground surface [11]. These approaches significantly increase the complexity, thickness, and tag's cost. In [12], a reflector is integrated with a tag slab to improve performance; however, its construction is bulky. Furthermore, various methods have been developed to improve the tag's performance, e.g., a thick slab with loss tangent [13], foam or air foam inserted between the tag and the tagged surfaces [14], [15], air gap separating two substrates [16], parasitic slab [17], and planar inverted-F antenna (PIFA) [18]. Unfortunately, these approaches increase the difficulty of the fabrication process. Folded-patch antenna has been proposed to enable miniaturization, with the shorting stubs mainly applied to shift the resonance frequency down [19], [22]. Further size reduction is realized by increasing the tag thickness to 3 mm [23] or by wrapping three conductor layers around two substrates of foam [24], [25]. However, the stub position significantly affects the tag's performance. Also, the structure is not practical for certain applications due to dual-layer structure and considerable thickness. In addition, utilization of adhesives to preserve the wrapped structure is questionable. Here, we aim at designing an UHF RFID tag antenna on a single slab using a flexible design approach, which is simple in construction, inexpensive, and convenient for mass production.

The main task of the tag antenna is to efficiently scatter the received power back from the interrogator. In this regard, ideal matching between the tag antenna and integrated circuit (IC) chip is essential to maximize the power transmission [26]. Generally, the impedance of the IC chip that is integrated with the tag's antenna has a high negative reactance (50 to 200 Ω) and low resistance (3 to 150 Ω). The simple structure of the folded dipole antenna boosts its utilization, but the backing metallic surface could affect the antenna's input impedance. In addition, a design of a compact UHF RFID dipole antenna with the size not exceeding 2, 500 mm^2 is a challenge because the compact low profile tag normally exhibits a high resonant frequency. To alleviate this issue, different approaches have been suggested for dipole antennas to attain matching with the reactance of the mounted IC chip, but maintaining compact size, such as nested loop [27] and T-match [28]. In [29], the outer strip lines are connected to C-shaped resonators where the presence of the outer strip lines assures matching to the IC chip's impedance. In [30], a folded dipole antenna has been proposed with symmetrical circular loads; the structure comprises an inner circular part surrounded by outer trace. Optimizing these loads can control the antenna impedance to match the capacitive reactance of the IC chip. The three-arm folded dipole antenna is incorporated with an additional element which assists in precise tune of the antenna's impedance [31]. The two meandered arms and feed line of modified dipole

fine tune tag's complex impedance [16]. The tag antenna in [32] consists of a matching loop connected directly to the folded dipole, which is combined with two patches. In [33], a loop antenna with two pairs of meandered lines can match the IC chip's impedance through a miniature shunt-stub. In general, a flexible low-profile UHF RFID tag antennas that can be readily matched to a variety of IC chip are highly desirable.

In this work, a novel miniature low-profile tag antenna is proposed for the UHF North American band (902 – 928 MHz), which utilized an interdigitated structure. The open stubs are mainly lengthened to increase the inductance of the tag antenna, where they work as inductors. This resulted in downward shifting of the tag's resonance frequency. The latter can be easily adjusted owing to the exclusion of the shorting walls or metallic vias, instead the flexible antenna structure ensures that an optimum reflection coefficient response can be obtained. The tag structure consists of horizontal strip lines, each loaded with seven identical open stubs. An inexpensive polytetrafluoroethylene (PTFE) substrate is employed to implement the tag. Unlike for many designs reported in the literature, no complex fabrication process is required. The proposed structure works effectively while mounted on metallic surfaces. The simulation results exhibit good agreement with the measurements.

II. ANTENNA DESIGN

A. ANTENNA STRUCTURE

This research proposes an interdigitated tag structure for miniaturization purposes. Fig. 1 depicts the geometry. The antenna is implemented on an inexpensive 1.5 mm thick PTFE slab (relative permittivity 2.55, loss tangent 0.0015 at 10 GHz). Two horizontal strip lines loaded with seven identical vertical open stubs and the feed lines form the tag antenna. The Higgs 4 strap chip is connected directly to the terminal of the feed lines in the middle of the antenna structure. The selected IC chip features a reading sensitivity P_{IC} of -20.5 dBm and an input impedance of $20.97 - j193.16\Omega$. The dimensions of the feed lines are precisely chosen to be suitable to mount a Higgs 4 strap chip. The width W_1 of feed lines is 4 mm, whereas the gap G between the feed lines is set to 3 mm. The loaded open stubs work as inductors resulting in increasing the inductive reactance of the antenna, which is useful for tuning the resonant frequency [34]. The open stubs can be characterized as lump elements L_{os} and C_{os} which are placed in parallel [35]. The inductance L_{os} of the each open stub is computed as [36],

$$L_{os} = 2L_i \left(\ln \left[\frac{2L_i}{W+t} \right] + 0.50049 + \left[\frac{W+t}{3L_i} \right] \right) \quad (1)$$

where L_i is the stub's length (3.21cm), W is the stub's width (0.3cm), and t is the thickness of the copper layer (0.0035cm). Thereby, the value of L_{os} is 23nH. The formed capacitance C_{os} between ground and each

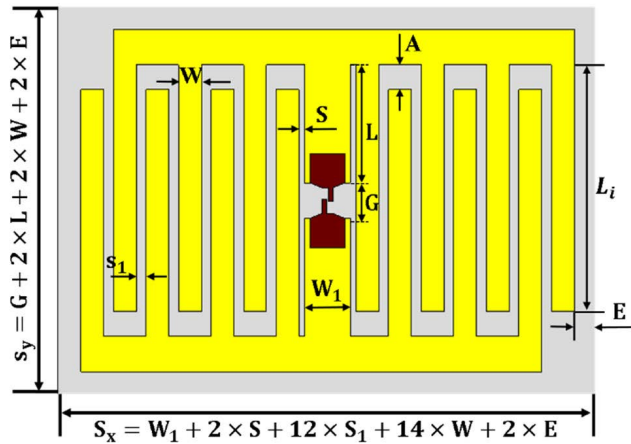


FIGURE 1. Geometry of suggested interdigitated structure $L = 15.6$, $W = 3$, $W_1 = 4$, $G = 3$, $A = 2.1$, $S = 0.2$, $S_1 = 0.4$, $L_f = 32.1$, $S_x = 55.2$, $S_y = 44.2$ (unit: mm, yellow color: copper, gray color: substrate, and maroon color: Higgs 4 strap chip).

stub is computed as [35],

$$C_{os} = \frac{\epsilon A_T}{h} \quad (2)$$

where A_T is the stub's size, h is the substrate's thickness, and $\epsilon = \epsilon_0 \epsilon_r$ with ϵ_r being the dielectric constant of the substrate. The capacitance C_{os} of each stub is $1.52 pF$. After the lumped elements values are determined, the open stub's impedance ($Z_{onestub}$) can be calculated as,

$$Z_{onestub} = \frac{j\omega L_{os}}{1 - \omega^2 C_{os} L_{os}} \quad (3)$$

The length L of the feed lines determines the length of the loaded open stubs which enables optimization. The tuning of the operating frequency is performed by adjusting L , which controls the length of the feed lines and the loaded open stubs, as well as the width W of the stubs. The parametric analysis of the space S_1 between the stubs, and the space A between the horizontal strip lines and the end of load open stubs is carried out to minimize the reflection coefficient response. Tuning of these parameters allows the antenna to realize an optimal impedance matching with the selected IC chip, where it works as an input impedance network. This structure has the flexibility to match any sort of IC because of the inductive coupling approach [37], [39]. The presented structure is designed to operate at the North American band (902 – 928 MHz).

B. DESIGN STAGES

The designed tag antenna is simulated and analyzes using CST Microwave studio. The Higgs 4 chip with two copper straps was precisely modeled through simulation, showed in [40]. When performing the simulation, the antenna was mounted on a $20cm \times 20cm$ perfect electrical conductor (PEC) surface with a total thickness of $1mm$. Notably, the tag performance in terms of reflection coefficient, gain, read patterns, realized gain, directivity, or read range,

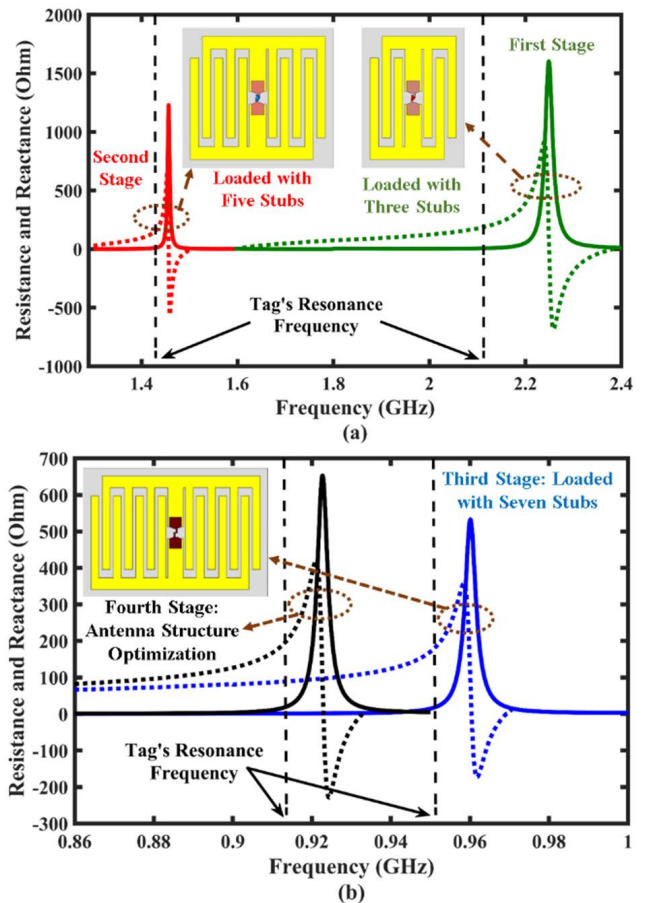


FIGURE 2. Input impedance of the tag antenna at (a) the first (loaded with three identical open stubs) and second stages (loaded with five identical open stubs), (b) the third (loaded with seven identical stubs) and final stages (tuning the dimensions of the antenna). (Solid line: resistance, dotted line: reactance).

is not affected by changing the thickness of the backing metallic surface [26].

The simulation starts with two horizontal strip lines loaded with three open stubs, and the Higgs 4 strap chip connected directly to the terminal of feed lines. At this stage, the resonant frequency of the structure was $2.116 GHz$ as shown in Fig. 2(a), which is considered too high for RFID implementations. Next, two extra open stubs were added to each horizontal strip line to increase the inductance of the tag antenna and shift the resonance downward. In this stage, each horizontal strip line was loaded with five identical open stubs. As shown in Fig. 2(a), the resonant frequency is shifted further downward to $1.436 GHz$. However, the operating frequency is still higher than the RFID band. Adding further open stubs results in shifting the resonant frequency to the RFID operation band (860 – 960 MHz) because of the increment in the antenna inductive reactance. In this stage, seven identical open stubs were connected to the horizontal strip line as seen in Fig. 2(b). Final optimization is performed by tuning the length L of feed line, the width W of the loaded open stubs, and the gaps A and S_1 , to have the antenna operate at the North American band

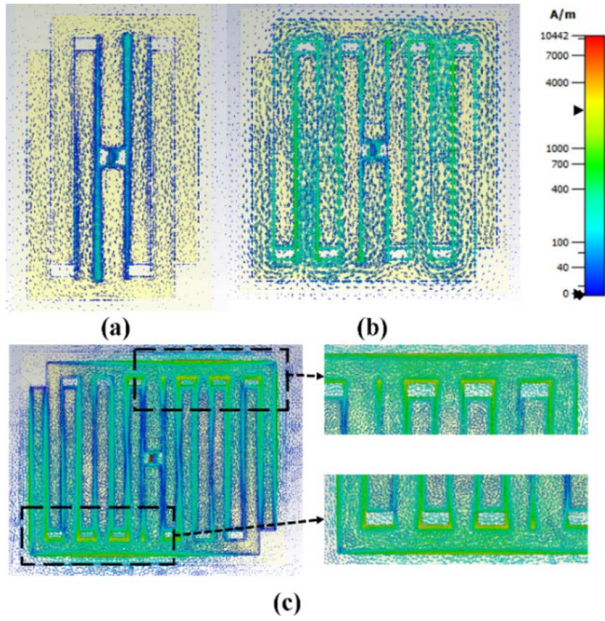


FIGURE 3. Tag antenna's surface current distribution at the resonance frequency for each design stage; (a) first stage, (b) second stage and (c) final stage.

(902 – 928 MHz) as seen in Fig. 2(b). The optimal match with the IC chip was achieved at 915 MHz. Additional inductive reactance is found at each stage when adding extra open stubs. This way, a minimum reflection coefficient value is realized, and a tag with an acceptable gain is obtained.

C. CURRENT ANALYSIS

This section presents the simulated surface current distribution. The analysis is performed while the tag is mounted on the upper surface of the PEC layer. Fig. 3(a) shows the results for the first version of the tag (horizontal strip lines loaded with three open stubs). The surface current is equal to 848 A/m. In the second stage as seen in Fig. 3(b), two additional open stubs are connected directly to each horizontal strip line (each horizontal strip line is loaded with five identical open stubs), where the inductance of the tag antenna increased and the increment of the surface current was observed to 2220 A/m. Fig 3(a) and 3(b) depicts the surface current at the corresponding resonant frequencies.

Fig. 3(c) shows the surface current of the proposed tag while mounted on PEC surface, at the operating frequency of 915 MHz. At this stage, after loading each horizontal strip line with extra two open stubs, the current path becomes longer, whereas each horizontal strip line is loaded with seven identical open stubs. The surface current is equal to 10442 A/m.

Incorporating additional open stubs result in the increase of the antenna inductance. Similarly, the operating frequency is brought down over the UHF RFID band, where the highest surface current density was observed on the feed lines, horizontal strip lines, and the connection area with the vertical

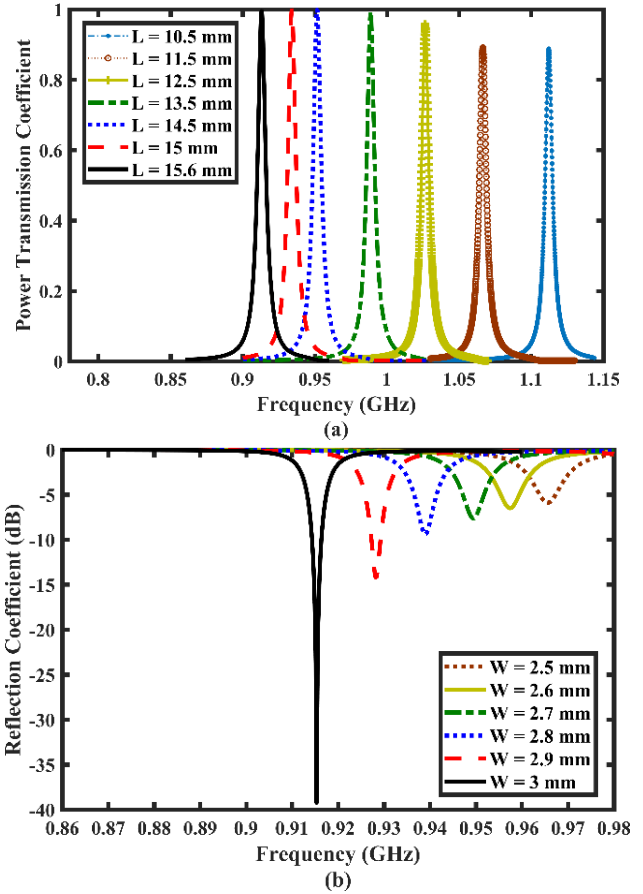


FIGURE 4. Parametric study: (a) computed power transmission coefficient of the proposed structure for various value of L , and fixed $W = 3$ mm, (b) simulated reflection coefficient response of the proposed structure for various values of W , and fixed $L = 15.6$ mm.

open stub. Thus, the overall structure of the proposed tag enables the adjustment of the resonant frequency. Further, increasing the number of loaded open stubs allows for minimizing the value of the reflection coefficient beyond -10 dB to obtain a conjugate match with the selected IC chip. The dimensional optimization of the feed lines, open stubs, and spaces between open stubs (A and S_1) has effectively shifted the operation frequency downward to 915 MHz.

D. PARAMETRIC STUDY

The CST software was used to perform parametric analysis of the proposed structure. The antenna response was optimized by tuning feed lines length L , which is directly related to the open stubs' length with a flexible tuning mechanism, open stubs width W , and the spaces A and S_1 . The main factor in shifting the resonant frequency downward is the increment of L as shown in Fig. 4(a). Adjusting the feed line length L from 10.5 to 15.6 mm brings the resonant frequency from 1.1036 GHz to 915 MHz at a rate of 36.98 MHz/mm for W fixed at 3 mm. Changing the open stubs width from 2.5 to 3.3 mm with L fixed at 15.6 mm, shifts the resonant frequency downward from 965 to 915 MHz at a rate of 100 MHz/mm as

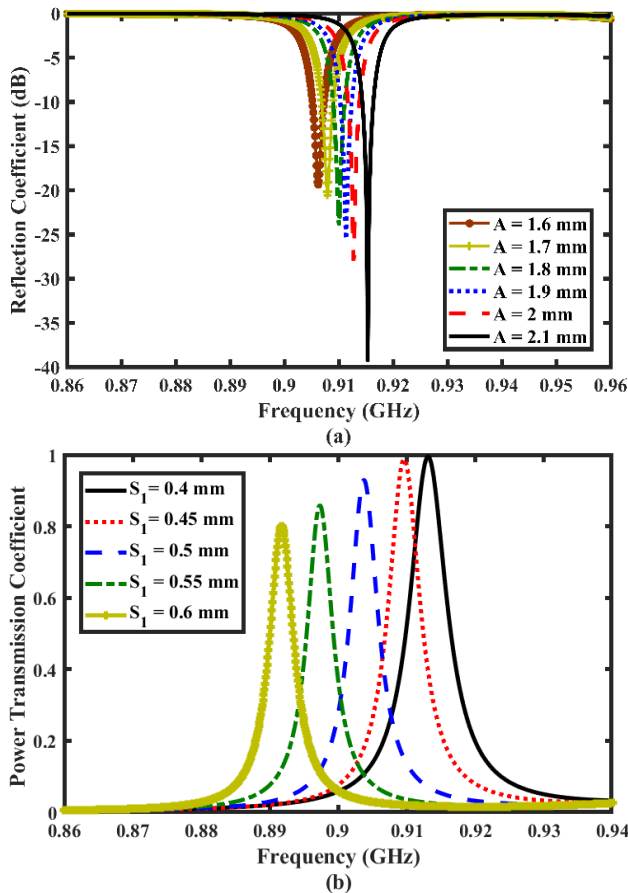


FIGURE 5. Parametric study: (a) simulated reflection coefficient response of the proposed structure: for various values of A, (b) computed power transmission coefficient for various values of S₁.

seen in Fig. 4(b). Further, the effect of A was studied where the length of the identical open stubs loaded on the horizontal strip lines is determined. A was adjusted to realize the best reflection response as shown in Fig. 5(a), with the achieved value of -39.2 dB . The parameter S₁ controls the strength of the mutual coupling between the open stubs, and facilitates obtaining a perfect impedance match by maximizing the power transmission coefficient ($\tau = 1$) as depicted in Fig. 5(b). Interdigitated structure’s performance is effectively improved by varying the value of S₁ and W as exhibited in Fig. 6. The G_a improved from -9.2 to -4.07 dB while changing S₁ value from 0.2 to 0.4 mm as seen in Fig. 6(a). Besides that, the tag’s performance in terms of realized gain is improved from -8.45 to -4.11 dB for varying W from 2.7 to 3 mm as seen in Fig. 6(b).

III. RESULTS AND DISCUSSION

This section presents the simulated and measured results of the proposed tag antenna. The Voyantic Tagformance Pro measurement system is utilized to obtain the realized gain G_r, tag sensitivity P_{tag}, and read range r of the presented structure. The measurement is conducted while the tag antenna is mounted on a 20cm × 20cm metal plate. Fig. 7(a) depicts the realized gain, which is -4.11 dB at 915 MHz according

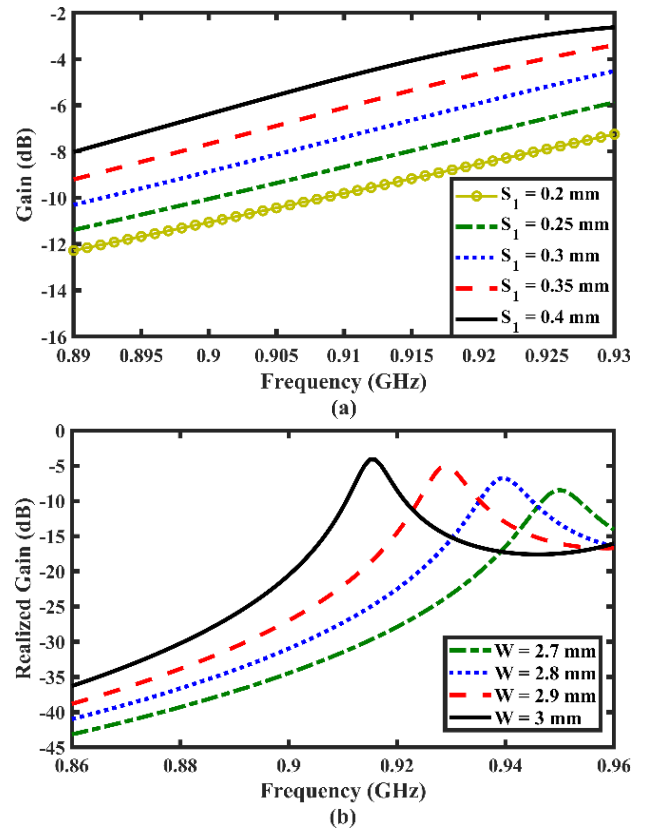


FIGURE 6. Parametric study: (a) simulated G_a of the proposed structure: for various values of S₁, (b) simulated G_r for various values of W.

to simulation, and -6.58 dB at 920 MHz, according to the measurement. The simulated G_r in the free space is -7.83 dB at 911 MHz. The difference between the measured and simulated results can be attributed to the IC chip impedance variations and etching/fabrication defects. Fig. 7(a) depicts the measured P_{tag} which is equal to -13.91 dBm at 920 MHz while being mounted on metallic surface.

The detection distance is computed using the Friis formula

$$r = (\lambda/4\pi)\sqrt{(P_{EIRP} \times G_r)/P_{th}} \quad (4)$$

where λ is the wavelength, P_{EIRP} refers to the RFID reader permitted output power (4 Watt), and P_{th} is the threshold power of chosen Higgs 4 strap chip. Fig. 7(b) shows the measured detection distance of the proposed tag antenna, which is 8.14 m on a metallic surface and 5 m in the free space. The computed detection distance is 10.88 m on the metal sheet. The backing metallic surface acts as a reflector that reduces back radiation of the tag and reflects the electromagnetic waves in-phase, thereby improving the tag’s performance in contrast to the free space condition.

Fig. 8 shows the read pattern of the proposed tag at 920 MHz. The tag is rotated in the x, y, and z axes during measurements to plot the measured read patterns in yz, xz, and xy planes while the reader is mounted at a fixed distance. The maximum detection distance appeared in the boresight direction ($\theta = 0^\circ$) and r is truncated beyond $\theta = \pm 90^\circ$

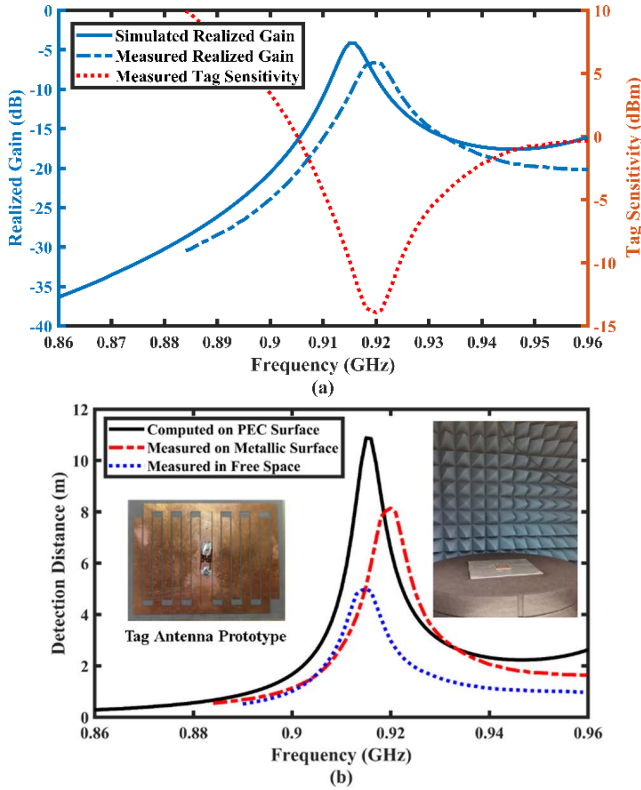


FIGURE 7. (a) Measured G_r and measured P_{th} the proposed structure on a $20\text{ cm} \times 20\text{ cm}$ metallic surface. (b) Measured and computed detection distance of the tag antenna on a metal surface.

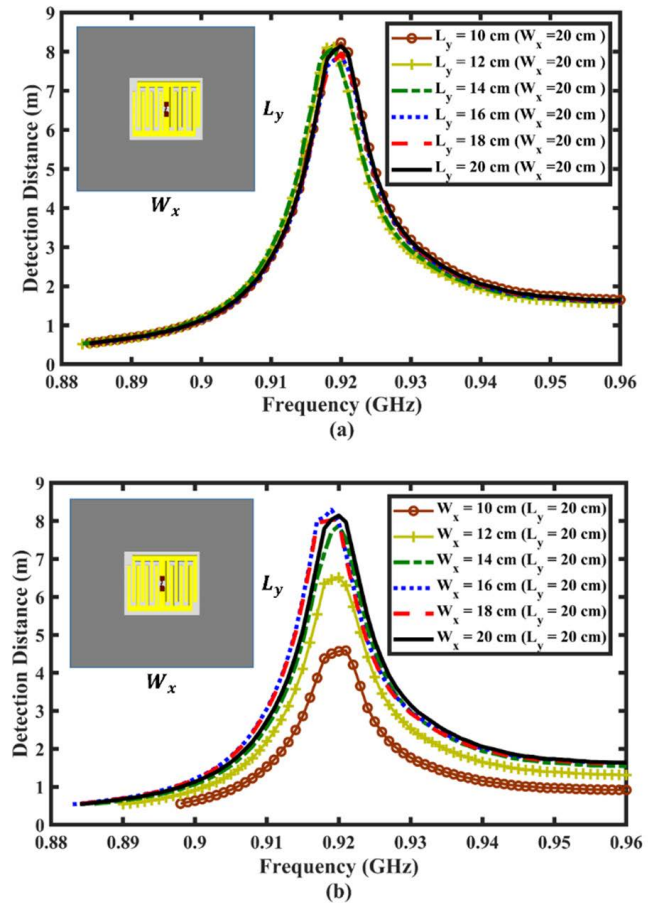


FIGURE 9. Measured detection distance of the suggested tag at various dimensions of (a) L_y from 10 cm to 20 cm for fixed W_x and (b) W_x from 10 cm to 20 cm for fixed L_y .

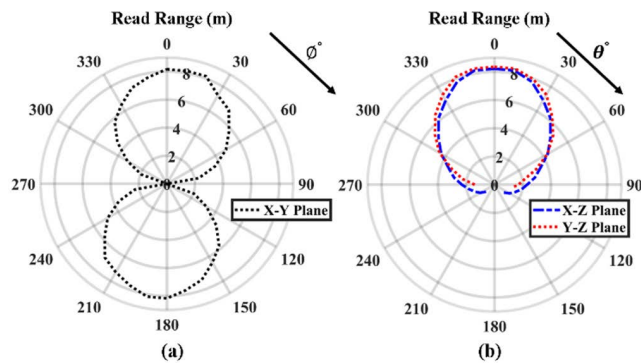


FIGURE 8. Measured detection pattern of the suggested tag on (a) xy and (b) yz and xz planes.

because of the existence of the metallic surface which operates as a reflector.

Fig. 9 illustrates the effect of varying dimensions L_y and W_x of the backing metallic surface on the tag's performance in terms of the reading distance. First, the length L_y of the metallic plate varies from 10 to 20 cm, whereas its width W_x is kept constant at 20cm, as shown in Fig. 9(a). The maximum detection distance is 8.14 m at the operating frequency. Notably, the tag's performance exhibited a similar response for various values of L_y . Subsequently, W_x varies from 10 to 20 cm for fixed $L_y = 20\text{ cm}$. The reading distance dropped to 4.56m when W_x changed from 20 to 10 cm due to the effect on the electrical flux strength at $\theta = 0^\circ$, which is only affected while varying W_x as shown in Fig. 9(b) [38].

These results indicate that the resonant frequency is still stable when the dimensions of metallic surface are changed, in other words, the RFID tag response to reader still appears over same frequency range while either L_y or W_x of metallic surface are varied. This feature is preferable for RFID metal-mountable implementations.

Table 1 shows a comparison of state-of-the-art metal-mountable UHF RFID tag antennas. Reference [41] reported a dual-layer tag antenna constructed from four PIFAs and the impedance matching obtained by shorting the stub lines to the ground. In [8], a novel folded dipole antenna with a symmetric dual-layer electromagnetic band gap (DLS-EBG), whereas its structure included an offset of vias. In these studies [8], [41], the general structure of the multi/double-layer tag antenna, is over 2 mm thick and contains metallic vias. Such construction is not desired for metal-mountable UHF tag antennas, and adjusting the input impedance/operation frequency is tedious. Likewise, their complex implementation affects the fabrication cost to a large extent. To overcome the metallic effect, the researchers in [14] used a foam spacer with a total thickness of 1 cm. The reported works in [18], [31], and [42] fabricated on a single-layer substrate and their structure included several metallic vias, which increase the fabrication complexity level and cost.

TABLE 1. Comparison Table of UHF RFID Metal Mountable Tags.

Ref.	Tag Dimension (mm^3)	Shorting Elements	Sim. G_r (dB)	P_{IC} (dBm)	Meas. r (m)
[8]	$72 \times 32 \times 6.8$	Vias	$G_a = 4.7$	-18	9
[14]	$51 \times 43 \times 1.58$	No	-	-8	4.5
[18]	$64 \times 64 \times 2$	Vias	$G_a = 0.3$	-17.4	10.2
[23]	$30 \times 30 \times 3$	stubs	1	-20	14.5
[31]	$69.5 \times 14 \times 1.5$	Vias	-	-15	2.4
[41]	$56 \times 26 \times 3.2$	Vias	-4.3	-15	4
[42]	$60 \times 45 \times 1.6$	Vias	$G_a = 1.9$	-	6.2
[43]	$40 \times 25 \times 3$	stubs	-0.9	-17.8	10.7
[44]	$30 \times 30 \times 3$	stubs	-3	-17.8	7.2
[45]	$40 \times 40 \times 1.6$	stubs	-8	-20	5.55
[46]	$42 \times 50 \times 1.6$	stubs	-	-20	5.2
This work	$55.2 \times 44.2 \times 1.5$	No	-4.11	-20.5	8.14

Moreover, a folding polyethylene terephthalate around the foam with shorting stubs was reported in [23], [43], and [46]. However, the highest realized gain is 1 dB for the design proposed in [23], but its thickness is over 2 mm, which is not preferable for metal mountable implementations. This is the reason why the structure proposed in this research does not include shorting walls or metallic vias. Our tag antenna is fabricated on a single-layer of PTFE slab, which allows for its straightforward deployment on metallic objects. In addition, the structure does not require any further complex fabrication processes, therefore, it is suitable for mass production.

IV. CONCLUSION

In this research, a novel low-profile metal-mountable UHF RFID tag antenna is proposed. The antenna is formed as an interdigitated structure comprising two horizontal strip lines loaded with seven identical open stubs. The measured detection distance is 8.14 m on a metal structure and 5 m in the free space. The proposed structure has a flexible tuning mechanism, low fabrication cost, and it is simple in construction. The aforementioned features make it suitable for mass production, and a variety of applications.

REFERENCES

[1] K. N. Salman, A. Ismail, R. S. A. R. Abdullah, and T. Saeedi, "Coplanar UHF RFID tag antenna with U-shaped inductively coupled feed for metallic applications," *PLoS ONE*, vol. 12, no. 6, Jun. 2017, Art. no. e0178388, doi: 10.1371/journal.pone.0178388.

[2] R. Abdulghafor, S. Turaev, H. Almohamedh, R. Alabdian, B. Almutairi, A. Almutairi, and S. Almutairi, "Recent advances in passive UHF-RFID tag antenna design for improved read range in product packaging applications: A comprehensive review," *IEEE Access*, vol. 9, pp. 63611–63635, 2021, doi: 10.1109/ACCESS.2021.3074339.

[3] M.-T. Nguyen, Y.-F. Lin, C.-H. Chen, C.-H. Chang, and H.-M. Chen, "Shorted patch antenna with multi slots for a UHF RFID tag attached to a metallic object," *IEEE Access*, vol. 9, pp. 111277–111292, 2021, doi: 10.1109/ACCESS.2021.3103177.

[4] I.-Y. Park and D. Kim, "Artificial magnetic conductor loaded long-range passive RFID tag antenna mountable on metallic objects," *Electron. Lett.*, vol. 50, no. 5, pp. 335–336, Feb. 2014, doi: 10.1049/el.2013.2671.

[5] D. Kim and J. Yeo, "Low-profile RFID tag antenna using compact AMC substrate for metallic objects," *IEEE Antennas Wireless Propag. Lett.*, vol. 7, pp. 718–720, 2008, doi: 10.1109/LAWP.2008.2000813.

[6] D. Hamzaoui, F. Djahli, T.-P. Vuong, T. Q. Van Hoang, and G. Kiani, "High gain long-read range AMC-backed tag antenna for European UHF RFID applications," *Microw. Opt. Technol. Lett.*, vol. 58, no. 12, pp. 2944–2948, Dec. 2016, doi: 10.1002/MOP.30185.

[7] D. Kim and J. Yeo, "Dual-band long-range passive RFID tag antenna using an AMC ground plane," *IEEE Trans. Antennas Propag.*, vol. 60, no. 6, pp. 2620–2626, Jun. 2012, doi: 10.1109/TAP.2012.2194638.

[8] X. Li, G. Gao, H. Zhu, Q. Li, N. Zhang, and Z. Qi, "UHF RFID tag antenna based on the DLS-EBG structure for metallic objects," *IET Microw., Antennas Propag.*, vol. 14, no. 7, pp. 567–572, Jun. 2020, doi: 10.1049/iet-map.2019.0780.

[9] B. Gao and M. M. F. Yuen, "Passive UHF RFID packaging with electromagnetic band gap (EBG) material for metallic objects tracking," *IEEE Trans. Compon., Packag., Manuf. Technol.*, vol. 1, no. 8, pp. 1140–1146, Aug. 2011, doi: 10.3109/15368378.2015.1077338.

[10] P. Kamalvand, G. K. Pandey, M. K. Meshram, and A. Mallahzadeh, "A single sided dual-antenna structure for UHF RFID tag applications," *Int. J. RF Microw. Comput.-Aided Eng.*, vol. 25, no. 7, pp. 619–628, Sep. 2015, doi: 10.1002/mmce.20900.

[11] L. Ukkonen, L. Sydänheimo, and M. Kivikoski, "Effects of metallic plate size on the performance of microstrip patch-type tag antennas for passive RFID," *IEEE Antennas Wireless Propag. Lett.*, vol. 4, pp. 410–413, 2005.

[12] L. Benmessaoud, T.-P. Vuong, M. C. E. Yagoub, and R. Touhami, "A novel 3-D tag with improved read range for UHF RFID localization applications," *IEEE Antennas Wireless Propag. Lett.*, vol. 16, pp. 161–164, 2017, doi: 10.1109/LAWP.2016.2565378.

[13] M. M. Bilgiç and K. Yeğin, "An HF/UHF dual mode RFID transponder antenna and HF range extension using UHF wireless power transmission," *Turkish J. Electr. Eng. Comput. Sci.*, vol. 24, pp. 3949–3960, 2016.

[14] M. A. Ennasar, I. Aznabet, O. EL Mrabet, and M. Essaaidi, "Design and characterization of a compact single layer modified S-shaped tag antenna for UHF-RFID applications," *Adv. Electromagn.*, vol. 8, no. 1, pp. 59–65, Mar. 2019.

[15] Y. F. Lin, M. J. Chang, H. M. Chen, and B. Y. Lai, "Gain enhancement of ground radiation antenna for RFID tag mounted on metallic plane," *IEEE Trans. Antennas Propag.*, vol. 64, no. 4, pp. 1193–1200, Apr. 2016, doi: 10.1109/TAP.2016.2526047.

[16] A. Hamani, M. C. E. Yagoub, T.-P. Vuong, and R. Touhami, "A novel broadband antenna design for UHF RFID tags on metallic surface environments," *IEEE Antennas Wireless Propag. Lett.*, vol. 16, pp. 91–94, 2017, doi: 10.1109/LAWP.2016.2557778.

[17] Y.-H. Niew, K.-Y. Lee, E.-H. Lim, F.-L. Bong, and B.-K. Chung, "Patch-loaded semicircular dipolar antenna for metal-mountable UHF RFID tag design," *IEEE Trans. Antennas Propag.*, vol. 67, no. 7, pp. 4330–4338, Jul. 2019, doi: 10.1109/TAP.2019.2905675.

[18] E.-S. Yang and H.-W. Son, "Dual-polarised metal-mountable UHF RFID tag antenna for polarisation diversity," *Electron. Lett.*, vol. 52, no. 7, pp. 496–498, Apr. 2016, doi: 10.1049/el.2016.0076.

[19] S.-Y. Ooi, P.-S. Chee, E.-H. Lim, Y.-H. Lee, and F.-L. Bong, "Stacked planar inverted-L antenna with enhanced capacitance for compact tag design," *IEEE Trans. Antennas Propag.*, vol. 70, no. 3, pp. 1816–1823, Mar. 2022, doi: 10.1109/TAP.2021.3118822.

[20] S.-M. Chiang, E.-H. Lim, P.-S. Chee, Y.-H. Lee, and F.-L. Bong, "Dipolar tag antenna with a top-loading inductive channel with broad range frequency tuning capability," *IEEE Trans. Antennas Propag.*, vol. 70, no. 3, pp. 1653–1662, Mar. 2022, doi: 10.1109/TAP.2021.3111093.

[21] N. Ripin, E.-H. Lim, F.-L. Bong, and B.-K. Chung, "Miniature folded dipolar patch with embedded AMC for metal mountable tag design," *IEEE Trans. Antennas Propag.*, vol. 68, no. 5, pp. 3525–3533, May 2020, doi: 10.1109/TAP.2020.2969814.

[22] Y.-H. Lee, E.-H. Lim, F.-L. Bong, and B.-K. Chung, "Loop-fed planar inverted-L antennas (PILAs) for omnidirectional UHF on-metal tag design," *IEEE Trans. Antennas Propag.*, vol. 68, no. 8, pp. 5864–5871, Aug. 2020, doi: 10.1109/TAP.2020.2990287.

[23] W. H. Ng, E. H. Lim, F. L. Bong, and B. K. Chung, "E-shaped folded-patch antenna with multiple tuning parameters for on-metal UHF RFID tag," *IEEE Trans. Antennas Propag.*, vol. 67, no. 1, pp. 1–9, Oct. 2018, doi: 10.1109/TAP.2018.2874795.

- [24] K. Thirappa, E.-H. Lim, F.-L. Bong, and B.-K. Chung, "Compact folded-patch with orthogonal tuning slots for on-metal tag design," *IEEE Trans. Antennas Propag.*, vol. 67, no. 9, pp. 5833–5842, Sep. 2019, doi: [10.1109/tap.2019.2920324](https://doi.org/10.1109/tap.2019.2920324).
- [25] W.-H. Ng, E.-H. Lim, F.-L. Bong, and B.-K. Chung, "Compact planar inverted-S antenna with embedded tuning arm for on-metal UHF RFID tag design," *IEEE Trans. Antennas Propag.*, vol. 67, no. 6, pp. 4247–4252, Jun. 2019, doi: [10.1109/TAP.2019.2911191](https://doi.org/10.1109/TAP.2019.2911191).
- [26] F. Erman, E. Hanafi, E.-H. Lim, W. A. W. M. Mahyiddin, S. W. Harun, M. S. A. Talip, R. Soboh, and H. Umair, "Low-profile folded dipole UHF RFID tag antenna with outer strip lines for metal mounting application," *Turkish J. Electr. Eng. Comput. Sci.*, vol. 28, no. 5, pp. 2643–2656, Sep. 2020, doi: [10.3906/elk-1912-45](https://doi.org/10.3906/elk-1912-45).
- [27] C. A. Balanis, *Antenna Theory Analysis and Design*. Hoboken, NJ, USA: Wiley, 1997.
- [28] T. Pumpoung and C. Phongcharoenpanich, "Design of wideband tag antenna for ultra-high-frequency radio frequency identification system using modified T-match and meander-line techniques," *Electromagnetics*, vol. 35, no. 5, pp. 340–354, Jul. 2015.
- [29] F. Erman, E. Hanafi, E.-H. Lim, W. A. W. M. Mahyiddin, S. W. Harun, H. Umair, R. Soboh, and M. Z. H. Makmud, "Miniature compact folded dipole for metal mountable UHF RFID tag antenna," *Electronics*, vol. 8, no. 6, p. 713, Jun. 2019, doi: [10.3390/electronics8060713](https://doi.org/10.3390/electronics8060713).
- [30] B. Yang and F. Quanyuan, "A folded dipole antenna for RFID tag," in *Proc. Int. Conf. Microw. Millim. Wave Technol. (ICMMT)*, Apr. 2008, pp. 1047–1049.
- [31] S. Genovesi and A. Monorchio, "Low-profile three-arm folded dipole antenna for UHF band RFID tags mountable on metallic objects," *IEEE Antennas Wireless Propag. Lett.*, vol. 9, pp. 1225–1228, 2010, doi: [10.1109/LAWP.2010.2103295](https://doi.org/10.1109/LAWP.2010.2103295).
- [32] F.-L. Bong, E.-H. Lim, and F.-L. Lo, "Compact folded dipole with embedded matching loop for universal tag applications," *IEEE Trans. Antennas Propag.*, vol. 65, no. 5, pp. 2173–2181, May 2017, doi: [10.1109/TAP.2017.2676776](https://doi.org/10.1109/TAP.2017.2676776).
- [33] X. Gao and Z. Shen, "UHF/UWB tag antenna of circular polarization," *IEEE Trans. Antennas Propag.*, vol. 64, no. 9, pp. 3794–3802, Sep. 2016.
- [34] S.-R. Lee, E.-H. Lim, F.-L. Bong, and B.-K. Chung, "Slotted circular patch with multiple loading stubs for platform insensitive tag," *IEEE Trans. Antennas Propag.*, vol. 66, no. 10, pp. 5072–5079, Oct. 2018, doi: [10.1109/TAP.2018.2858149](https://doi.org/10.1109/TAP.2018.2858149).
- [35] F. Giannini and C. Paoloni, "Broadband lumped equivalent circuit for shunt-connected radial stub," *Electron. Lett.*, vol. 24, no. 22, pp. 485–487, 1986.
- [36] H. M. Greenhouse, "Design of planar rectangular microelectronic inductors," *IEEE Trans., Hybrids, Packag.*, vol. HP-10, no. 2, pp. 101–109, Jun. 1974, doi: [10.1109/TPHP.1974.1134841](https://doi.org/10.1109/TPHP.1974.1134841).
- [37] A. R. H. Alhawari, A. Ismail, A. S. A. Jalal, R. S. A. R. Abudullah, and M. F. A. Rasid, "U-shaped inductively coupled feed radio frequency identification tag antennas for gain enhancement," *Electromagnetics*, vol. 34, no. 6, pp. 487–496, Aug. 2014, doi: [10.1080/02726343.2014.922767](https://doi.org/10.1080/02726343.2014.922767).
- [38] F. Erman, E. Hanafi, E.-H. Lim, W. A. W. M. Mahyiddin, S. W. Harun, H. Umair, and R. Soboh, "U-shaped inductively coupled feed UHF RFID tag antenna with DMS for metal objects," *IEEE Antennas Wireless Propag. Lett.*, vol. 19, no. 6, pp. 907–911, Jun. 2020, doi: [10.1109/LAWP.2020.2981960](https://doi.org/10.1109/LAWP.2020.2981960).
- [39] F. Erman, S. Koziel, E. Hanafi, R. Soboh, and S. Szczepanski, "Miniaturized metal-mountable U-shaped inductive-coupling-fed UHF RFID tag antenna with defected microstrip surface," *IEEE Access*, vol. 10, pp. 47301–47308, 2022, doi: [10.1109/ACCESS.2022.3171243](https://doi.org/10.1109/ACCESS.2022.3171243).
- [40] (2016). *Higgs 4 RFID IC | Alien Technology*. Accessed: Oct. 8, 2018. [Online]. Available: <https://www.alientechnology.com/products/ic/higgs-4/>
- [41] J. Zhang and Y. Long, "A dual-layer broadband compact UHF RFID tag antenna for platform tolerant application," *IEEE Trans. Antennas Propag.*, vol. 61, no. 9, pp. 4447–4455, Sep. 2013, doi: [10.1109/TAP.2013.2269472](https://doi.org/10.1109/TAP.2013.2269472).
- [42] W. Zeng, J. Zhao, B. Ke, and Q. Wu, "Compact microstrip RFID tag antenna mountable on metallic objects," *Proc. Eng.*, vol. 16, pp. 320–324, Jan. 2011, doi: [10.1016/j.proeng.2011.08.1090](https://doi.org/10.1016/j.proeng.2011.08.1090).
- [43] C.-W. Moh, E.-H. Lim, F.-L. Bong, and B.-K. Chung, "Miniature coplanar-fed folded patch for metal mountable UHF RFID tag," *IEEE Trans. Antennas Propag.*, vol. 66, no. 5, pp. 2245–2253, May 2018.
- [44] F.-L. Bong, E.-H. Lim, and F.-L. Lo, "Flexible folded-patch antenna with serrated edges for metal-mountable UHF RFID tag," *IEEE Trans. Antennas Propag.*, vol. 65, no. 2, pp. 873–877, Feb. 2017, doi: [10.1109/TAP.2016.2633903](https://doi.org/10.1109/TAP.2016.2633903).
- [45] W.-H. Ng, E.-H. Lim, F.-L. Bong, and B.-K. Chung, "Folded patch antenna with tunable inductive slots and stubs for UHF tag design," *IEEE Trans. Antennas Propag.*, vol. 66, no. 6, pp. 2799–2806, Jun. 2018, doi: [10.1109/TAP.2018.2821702](https://doi.org/10.1109/TAP.2018.2821702).
- [46] S.-R. Lee, E.-H. Lim, F.-L. Bong, and B.-K. Chung, "Slotted folded patch antenna with double-T-slots for platform-insensitive UHF tag design," *IEEE Trans. Antennas Propag.*, vol. 67, no. 1, pp. 670–675, Jan. 2019, doi: [10.1109/TAP.2018.2878346](https://doi.org/10.1109/TAP.2018.2878346).



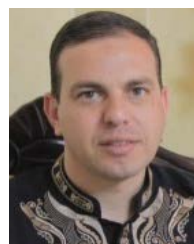
FUAD ERMAN was born in Palestine. He received the B.Eng. degree in electronics and communications engineering from Al-Baath University, in 2013, the M.Eng.Sc. degree in communication and network engineering from the University of Putra Malaysia, in 2017, and the Ph.D. degree in electrical engineering from the University of Malaya, in 2020. He is currently working as a Postdoctoral Researcher with the Engineering Optimization and Modeling Center (EOMC), Department of Electrical Engineering, Reykjavik University, Iceland. His current research interests include RFID antennas, RFID sensors, wearable antennas, and fiber lasers.



DALIA MANSOUR received the B.S. degree in communication engineering from Palestine Technical University–Kadoorie, Palestine, in 2018, and the M.S. degree in electronics and computer engineering from Al-Quds University, Palestine, in 2021. She is currently a Communication Engineer in Tulkarm, Palestine. Her research interests include RFID technology, tag antennas, and the IoT.



MOHAMMAD KOUALI received the B.Sc. degree in electronics engineering from Al-Quds University (AQU), Palestine, and the M.Sc. and Ph.D. degrees from the Ecole Polytechnique de L'Université de Nantes, France. He is currently an Assistant Professor with the Department of Electronics and Communication Engineering, AQU. His research interests include computational electromagnetics, radar remote sensing, and antennas and radio wave propagation.



ARAFAT SHABANEH received the B.S. degree from Palestine Polytechnic University, Palestine, in 2006, the M.S. degree in communication engineering from International Islamic University Malaysia, Malaysia, 2011, and the Ph.D. degree in the area of optical sensors based on nanometers from Universiti Putra Malaysia, Malaysia, in 2015. He worked with the Centre of Excellence for Wireless and Photonic Network, Universiti Putra Malaysia. He is currently a Lecturer with the Department of Communication Technology, College of Engineering and Technology, Tulkarm, Palestine. His research interests include optical sensors, optical communication systems, and nanotechnology.



LEIFUR LEIFSSON received the bachelor's and master's degrees in mechanical engineering from the University of Iceland, Reykjavik, Iceland, in 1999 and 2000, respectively, and the Ph.D. degree in aerospace engineering from Virginia Tech, Blacksburg, VA, USA, in 2006. He is currently an Associate Professor in aerospace engineering with Purdue University, West Lafayette, IN, USA. His research interests include computational modeling, optimization, uncertainty quantification of

engineered systems with an emphasis on methods for multifidelity modeling and machine learning, aerodynamic shape optimization, aerodynamic flutter, model-based nondestructive evaluation, microwave devices, and food-energy-water nexus.



ENG-HOCK LIM (Senior Member, IEEE) was born in Malaysia. He received the B.Sc. degree in electrical engineering from the National Taiwan Ocean University, in 1997, the M.Eng. degree in electrical and electronic engineering from Nanyang Technological University, in 2000, and the Ph.D. degree in electronic engineering from the City University of Hong Kong, in 2007. He is currently a Professor with Universiti Tunku Abdul Rahman (UTAR). He was the Founding Chair of

the IEEE Malaysia Council on RFID. He served as an Associate Editor for the IEEE TRANSACTIONS ON ANTENNAS AND PROPAGATION, from 2013 to 2016. He is currently serving as the Associate Editor for the IEEE JOURNAL OF RADIO FREQUENCY IDENTIFICATION. Since April 2021, he has been a Distinguished Lecturer of the IEEE Council on RFID. He is a fellow of the Academy of Sciences Malaysia and the ASEAN Academy of Engineering and Technology. His current research interests include RFID antennas, smart and re-configurable antennas, and multifunctional antennas.



SLAWOMIR KOZIEL (Fellow, IEEE) received the M.Sc. and Ph.D. degrees in electronic engineering from the Gdansk University of Technology, Poland, in 1995 and 2000, respectively, the M.Sc. degrees in theoretical physics and in mathematics, in 2000 and 2002, respectively, and the Ph.D. degree in mathematics from the University of Gdansk, Poland, in 2003.

He is currently a Professor with the Department of Engineering, Reykjavik University, Iceland. His research interests include CAD and modeling of microwave and antenna structures, simulation-driven design, surrogate-based optimization, space mapping, circuit theory, analog signal processing, evolutionary computation, and numerical analysis.



EFFARIZA HANAFI (Member, IEEE) received the B.Eng. degree (Hons.) in telecommunications from The University of Adelaide, Adelaide, SA, Australia, in 2010, and the Ph.D. degree in electrical and electronic engineering from the University of Canterbury, Christchurch, New Zealand, in 2014. She joined the University of Malaya, Kuala Lumpur, Malaysia, where she is currently a Senior Lecturer in electrical engineering. She has authored or coauthored journal articles in

ISI-indexed publications and refereed conference papers. Her research interests include multiple antennas systems, RFID, cognitive radio networks, cooperative communications in wireless communications, the Internet of Things, and 5G networks.

...